ADVANCED FUNCTIONAL MATERIALS
www.afm-journal.de

www.MaterialsViews.com

Versatile Graphene-Promoting Photocatalytic Performance of Semiconductors: Basic Principles, Synthesis, Solar Energy Conversion, and Environmental Applications

Wenguang Tu, Yong Zhou, and Zhigang Zou**

Graphene-semiconductor nanocomposites, considered as a kind of most promising photocatalysts, have shown remarkable performance and drawn significant attention in the field of photo-driven chemical conversion using solar energy, due to the unique physicochemical properties of graphene. The photocatalytic enhancement of graphene-based nanocomposites is caused by the reduction of the recombination of electron-hole pairs, the extension of the light absorption range, increase of absorption of light intensity, enhancement of surface active sites, and improvement of chemical stability of photocatalysts. Recent progress in the photocatalysis development of graphene-based nanocomposites is highlighted and evaluated, focusing on the mechanism of graphene-enhanced photocatalytic activity, the understanding of electron transport, and the applications of graphene-based photocatalysts on water splitting, degradation or oxidization of organic contaminants, photoreduction of CO_2 into renewable fuels, toxic elimination of heavy metal ions, and antibacterial applications.

1. Introduction

Graphene, a single two-dimensional nanosheet of sp^2 hybridized carbon, is a zero bandgap semiconductor, possessing unique electrical properties such as massless fermions, ballistic electronic transport, and ultrahigh electron mobility (200 000 cm^2 V^{-1} s^{-1}).[1–6] Since graphene was obtained from simple mechanical cleavage in 2004,[1] the other unique properties such as high flexible structure,[7] large surface area (2630 m^2/g),[8] high transparency (optical transmittance is 97.7%),[9] and high thermal conductivity (≈5000 W m^{-1} K^{-1})[10,11] were also discovered. Due to these fascinating properties, graphene has drawn considerable attention to conduct its fundamental studies and explore its potential applications in the field of material science.

In order to grow graphene and its derivatives, versatile methods have been developed during past several years. The strategies are generally classified into two approaches: "top-down" and "bottom-up". The "bottom-up" epitaxial growth method includes chemical vapor deposition[12–16] and organic synthesis.[17–19] The "bottom-up" growth of graphene from small molecules affords an attractive strategy, not only producing large-size (up to several centimeters) and high-quality graphene but also adjusting its morphology and structure.[12,15,17,20] The "top-down" growth of graphene is mostly based on the exfoliation of bulk graphite, involving the mechanical exfoliation of graphite,[1,21,22] electrochemical expansion of graphite,[23] the longitudinal 'unzipping' of carbon nanotubes (CNTs),[24–26] and chemically derived graphene by reducing graphene oxide (GO), which is an easy strategy to produce graphene with a large scale and at a low cost although graphene derived from reducing GO inevitably introduces oxygen-containing groups and defects.[27,28] GO is usually synthesized through the oxidation of graphite using oxidants including concentrated sulfuric acid, nitric acid and potassium permanganate based on Hummers method.[27,28] Versatile methods for fabricating graphene thus offer tremendous opportunities to extend its applications in field-effect transistors,[1] memory devices,[29] photovoltaic devices,[30] sensors,[31] making patterns on graphene[32], energy storage/generation devices,[33] solar cells,[34] polarizer,[35] and others,[36] as systematically described in most recent reviews.[37–45]

Here, we highlight and evaluate recent progress in the photocatalysis development of graphene-based nanocomposites. The photocatalytic enhancement of graphene-based nanocomposites is caused by the reduction of the recombination of electron-hole pairs, the extension of the light absorption range, increase of absorption of light intensity, enhancement of surface active sites, and improvement of chemical stability of photocatalysts. This article begins with brief description of the basic principle of graphene-enhanced photocatalytic activity. We then introduce the various methods of design and fabrication of graphene-based nanocomposites. Finally, recent photocatalytic

Dr. W. Tu, Prof. Y. Zhou
Key Laboratory of Modern Acoustics
MOE, Institute of Acoustics
Department of Physics
Nanjing University
Nanjing 210093, P. R. China
E-mail: zhouyong1999@nju.edu.cn
Dr. W. Tu, Prof. Y. Zhou, Prof. Z. Zou
National Laboratory of Solid State Microstructures
School of Physics
Eco-materials and Renewable
Energy Research Center (ERERC)
Nanjing University
Nanjing 210093, P. R. China
E-mail: zgzou@nju.edu.cn

DOI: 10.1002/adfm.201203547

applications are summarized, including water splitting, photodegradation or photooxidization of organic contaminants, photoreduction of CO_2 into hydrocarbon solar fuel, toxic elimination of heavy metal ions, and antibacterial applications.

2. Basic Principles of Photocatalytic Enhancement for Graphene-Based Nanocomposites

The conversion of solar energy to chemical energy using photocatalysis reaction has attracted increasing attention since the 1970s, because it is one promising technology to solve energy shortage and environmental related problems, which are the worsening worldwide problems and the great challenges for human in the 21st century. In the photocatalytic processes, a flux of photons absorbed by semiconductor excites electrons from the valence band (VB) to the conduction band (CB), leaving an equal numbers of holes in the VB. The photogenerated electron-hole pairs separate from each other and vigorously migrate to catalytically active sites at semiconductor surface where they reduce the electron acceptors or oxidize the donor species. Through the chemical transformations, the abundant solar energy in the world can thus be effectively stored and utilized. However, electron-hole pairs may also recombine and dissipate as heat easily before they arrive at the surface, diminishing the efficiency of photocatalytic activity, which is one notorious and fundamental issue.

Along with the continuing in depth analysis of photocatalytic processes, efficient photocatalytic activity of semiconductor photocatalysts should benefit from: (1) the bandgap of semiconductors allows absorption of incident light across the region of solar spectrum to generate the electron-hole pairs; (2) electron-hole pairs separate effectively from each other and arrive at the semiconductor surface, minimizing the recombination of electron-hole pairs; (3) the photocatalysts supply adequate quality and quantity of active sites, offering more adsorption sites and photocatalytic reaction centers; and (4) the bottom of the CB should locate at a more negative potential than the reduction potential, and the top of the VB must have a more positive potential than the oxidation potential,[46] so that redox reactions are thermodynamically feasible. However, it is difficult to satisfy these harsh terms for semiconductor photocatalysts simultaneously. For example, a large bandgap (3.2 eV) of anatase TiO_2 responds to ultraviolet (UV) light which makes up only about 3–5% of solar spectrum, though it is the most widely-researched photocatalyst. Owing to relatively narrow band gap (2.4 eV), CdS is also one of most studied visible light-catalyzed photocatalyst; however, it suffers from the low separation efficiency of electron–hole pairs and photocorrosion during light irradiation.[47,48] The energy losses related to charge transport and electron-hole recombination also significantly destroy the photocatalytic performance.

Graphene, a two-dimensional honeycomb-like network of carbon atoms, has been used as a support for fabricating various nanohybrids with semiconductors. The hybrid of graphene and semiconductors can assist the settlement of those problems during the photocatalytic process[49–62]: (1) graphene is widely recognized to serve as a good electron collector and transporter to efficiently hinder recombination of photogenerated electron-hole pairs (**Figure 1**),[49–55] resulting in high performance of photocatalytic activity, due to its unique physicochemical properties.[51,60–62] For thermodynamically feasible electron transport from semicondutors to graphene, the conduction band of semiconductors should be smaller than the

Yong Zhou studied chemistry and physics at the University of Science and Technology of China (USTC), received his Ph.D. degree there in 2000. After working in Kyoto University in 2000–2001, Max Planck Institute of Colloids and Interfaces in 2002–2003, the National Institute of Materials Science (NIMS, Japan) in 2003–2004, National Institute of Advanced Industrial Science and Technology (AIST, Japan) in 2004–2008, and National University of Singapore (NUS) in 2008–2009, he joined as a full professor in the Eco-materials and Renewable Energy Research Center (ERERC), School of Physics, National Laboratory of Solid State Microstructures, Nanjing University, China. His research now focuses on design and fabrication of solar-light driven clean energy materials for photocatalysis and flexible solar cells.

Zhigang Zou received his Ph.D. degree in 1996 from the University of Tokyo. He worked as a researcher in AIST in Japan during 1996–2002. He became a Cheung Kong Scholars professor of the Department of Physics and a leader of ERERC in Nanjing University since 2003. His research interests include superconductor, photocatalysis and photoelectrochemisty for solar hydrogen production.

Wenguang Tu obtained his BS degree in 2010 from Southwest University, China. He is pursuing his PhD degree under the guidance of Prof. Yong Zhou in ERERC, School of Physics, National Laboratory of Solid State Microstructures, Nanjing University, China. His current research involves the synthesis of graphene-based nanomaterials for photocatalysis application.

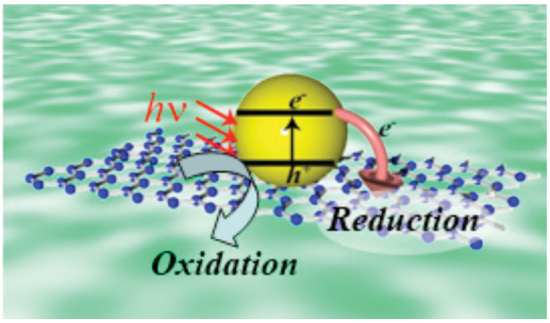

Figure 1. Schematic illustration of graphene as an electron collector and transporter to for photo-driven redox reaction over photocatalysts.

work function of graphene. Typically, the work function for graphene is ≈4.42 eV[63,64] and the conduction band of TiO_2 is around −4.21 eV (vs. vacuum).[65] Such energy levels are beneficial for transporting photogenerated electrons from TiO_2 to graphene. Consequently, understanding of the band edge positions of semiconductors relative to the work function of graphene can guide one to rationally design graphene-based photocatalysts. (2) The hybrid of graphene and semiconductors such as TiO_2[60,61] and CdS[62] can increase the absorption of light intensity and extend the light absorption range, so more efficient utilization of the solar energy is obtained. Typically, graphene-TiO_2 nanoparticle composites usually exhibit a red shift of the band-edge and a significant reduction of the bandgap, which may be caused by the interaction between unpaired π electrons of graphene and Ti atoms[60] and the chemical bonding (Ti-O-C bond) between TiO_2 and graphene.[61] (3) The large surface area of flexible graphene as supporting matrices usually leads to the increase of the surface area of the graphene-based nanocomposites, which supply more surface active sites and increase the adsorption of reactants. Meanwhile, the hybridization process prevents not only the restacking of the single-layer graphene, but also the aggregation of semiconductor particles such as CdS quantum dots.[51]

Several techniques and measurements such as photoluminescence (PL) spectroscopy, time-resolved fluorescence spectroscopy, photocurrent response data, electrochemical impedance spectra (EIS) measurement, and electron spin resonance (ESR) spectrum are utilized to study and monitor the impact of incorporated graphene on the separation and transportation of photogenerated electron-hole pairs under light irradiation. Graphene as an electron acceptor supplies as additional nonradiative delay channel for the transfer of electrons from semiconductors to graphene, resulting in the PL quenching.[50,55,66] Time-resolved fluorescence spectroscopy monitors the electron transfer between semiconductors and graphene through the study of emission lifetimes of graphene-based composites.[51,67] Photocurrent measurement can help understand the role of sufficiently compact interfacial contact between graphene and semiconductors on enhancing the lifetime of electron-hole pairs.[53,64,67] Nyquist plots obtained by EIS measurement supply the information about charge transfer resistance in solid-state interface layer and the charge transfer resistance at the contact interface between electrode and electrolyte solution.[61,68,69] The ESR spectrum may confirm the accumulation of the radical species such as hydroxyl radical (•OH), and superoxide radicals ($\bullet O_2^-$), when graphene is incorporated with semiconductors.[70,71]

3. Synthesis of Graphene-Based Photocatalysts

Graphene is a desirable two-dimensional supporting matrix for various semiconductor photocatalysts, as listed in **Table 1**. In order to achieve sufficient performance of graphene-based photocatalysts, it is essential to anchor the semiconductor species densely and uniformly with graphene to promote electron transfer in photocatalytic reactions. Thus, it must avoid the notorious aggregation problem of graphene owing to the intrinsic incompatibility between graphene and inorganic materials and balance the maximizing contact with the semiconductor species while minimizing incident light absorption by graphene. The two general strategies of synthesis of graphene-based photocatalysts involve solution mixing and in situ growth, as schematically illustrated in **Figure 2**.

3.1. Solution Mixing

Solution mixing is a direct and simple approach to prepare graphene-based photocatalysts by solution mixing of GO (or graphene) and semiconductors (Figure 2a,b).[72,73] Commercialized TiO_2 (P25) and GO nanocomposites were prepared using a simple colloidal blending method through sonicate and stirring,[73] during which the possible chemical interaction between surface hydroxyl groups of TiO_2 and functional groups of GO leads to the form of Ti–O–C bonds in the nanocomposites. However, only part of P25 nanoparticles were anchored to GO nanosheets through this method, as P25 is not dispersed in deionized water very well. The hydrothermal route-assisted solution mixing allows to obtain good reduction of GO and the prefect interfacial contact of graphene and semiconductors.[61,70] A two-phase method was proposed to prepare graphene–TiO_2 nanorod nanocomposites.[72] With mixing of the aqueous solution of GO with the toluene solution of oleic acid-capped anatase TiO_2 nanorods, TiO_2 nanorods were uniformly self-assembled on the GO at the water/toluene interface with easy control of the ratio of GO/TiO_2. The similar water/oil or oil/water system was also developed to prepare Ag/AgX/GO (X = Br, Cl) nanocomposites.[74,75]

Electrostatic interaction is utilized as the driving force for self-assembling photocatalysts on graphene or GO. Surface modification of the nanoparticles or graphene can increase the charge density for controlling the self-assembly process. TiO_2 nanoparticles wrapped by graphene were prepared by mixing positively charged amine-functionalized amorphous TiO_2 nanoparticle dispersion and negatively charged GO suspension, followed by a one-step GO reduction and TiO_2 crystallization via hydrothermal treatment.[60] Strongly coupled nanocomposites of layered titanate and reduced graphene oxide (RGO) was synthesized by electrostatically derived self-assembly between negatively charged RGO nanosheets and positively charged TiO_2

Table 1. Recent reports of graphene-based photocatalysts for solar energy conversion and environment applications.

Photocatalysts / Applications	TiO_2	ZnO	CdS	C_3N_4	Others
Water splitting	98, 101, 192-195, 68, 97, 102, 196-200		104, 224, 62, 103, 164, 194, 223	66	MoS_2,[226] $Zn_xCd_{1-x}S$[106], $Sr_2Ta_2O_7$[105], Cu_2O[107], WO_3[227], $BiVO_4$[53], $BiVO_4$-G-Ru/$SrTiO_3$:Rh[108], α-Fe_2O_3/G/$BiV_{1-x}Mo_xO_4$[228], $AgPO_4$/Ag/AgBr[229], CdS/Oxide (Oxide = ZnO, Al_2O_3)[230]
Degradation or oxidization of organic contaminants	54, 60, 61, 70, 72, 73, 76, 110, 112, 120, 121, 123-125, 128, 129, 135, 144-147, 156, 157, 159, 160, 168, 169, 201-205, 71, 78, 79, 82, 109, 114, 116, 117, 131, 132, 134, 137, 138, 149, 151, 153, 154, 158, 161, 173, 206-211. G-TiO_2-Fe_3O_4[212], (YF_3:Yb^{3+}, Tm^{3+})-P25-G[213]	126, 215, 118, 122, 127, 141, 148, 166, 216-221, Ag-ZnO-G[165]	83, 143, 154, 163, 174, 225	150	Au[241], Cu_2O[119, 142], CuO[152], SnO_2[132, 231, 232], WO_3[233], SiC[167], CNTs[111], $Mg(OH)_2$[90], CuS[234], ZnS[115, 175], ZnSe[139], $BiVO_4$[113, 235], Bi_2WO_6[84, 155], Bi_2MoO_6[136, 236], $InNbO_4$[133], $La_2Ti_2O_7$[91], BiOCl[238], BiOBr[91-93, 237], Ag/AgX (X=Br, Cl)[74, 75, 130], $AgPO_4$[178, 179], ferrites (MFe_2O_4, M = Mn, Zn, Cu, Co and Ni)[69, 85-89], ZnWO4[239], ZnO@ZnS[240], CdS/Oxide (Oxide=ZnO, Al_2O_3)[230]
CO_2 conversion	55, 77, 184, 80				
reduction of metal ions	187, 214, 117	186, 222	188		
Antibacterial application	189, 191				WO_3[190]

Symbol '___' refers to solution mixing method. No symbol refers to in situ growth method. '---' refers to none of both methods

nanosols, which was then followed by a phase transition of the anatase TiO_2 component into layered titanate.[76] The composite formation with RGO nanosheets is effective not only in promoting the phase transition of anatase TiO_2 nanosols, but also in improving the thermal stability of the layered titanate, indicating the role of RGO nanosheets as an agent for directing and stabilizing layered structures. Robust hollow spheres consisting of molecular-scale alternating titania ($Ti_{0.91}O_2$) nanosheets and graphene nanosheets as building blocks were successfully fabricated by a layer-by-layer assembly technique on poly(methyl methacrylate) (PMMA) beads as sacrificial templates using a microwave irradiation technique to simultaneously remove the template and reduce GO into graphene (**Figure 3**).[77] The molecular scale, two-dimensional contact of $Ti_{0.91}O_2$ nanosheets and graphene nanosheets in the hollow spheres is distinctly different from the prevenient graphene-based TiO_2 nanocomposites prepared by the simply integration of TiO_2 and graphene nanosheet (**Figure 4**).

3.2. In Situ Growth

In situ growth approach has been considered as one of the best methods to synthesize graphene-based photocatalysts (Figure 2c and 2d). GO or RGO is usually selected as the starting materials, in which oxygen-containing functional groups on the surface of GO or RGO act as the nucleation sites for in situ growing and anchoring inorganic nanocrystals. A graphene/TiO_2 nanocrystals hybrid was prepared by a two-step

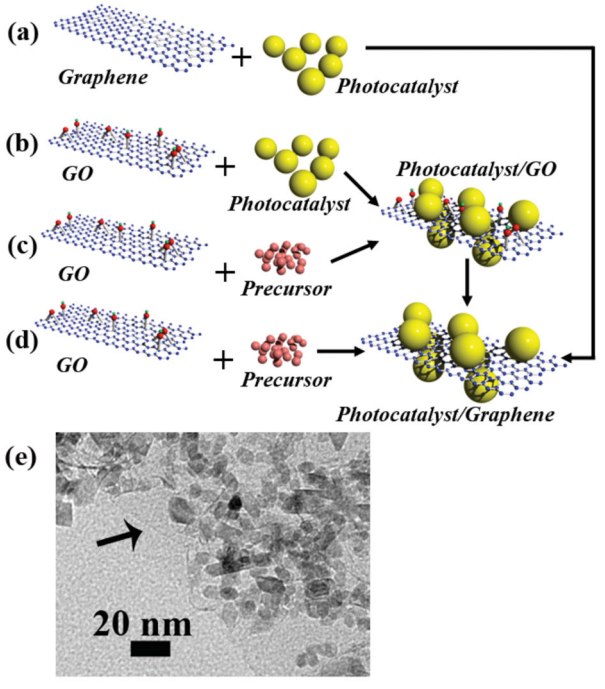

Figure 2. Diagram of the a,b) solution mixing and c,d) in situ growth for synthesis of graphene-based photocatalysts. e) Typical TEM image of graphene-TiO_2 nanocomposite, showing the dispersion of the nanoparticle on graphene. The arrowhead indicates the graphene in (e).

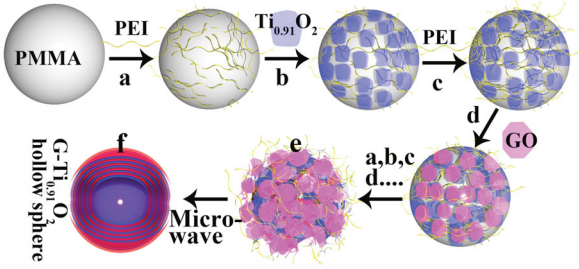

Figure 3. Schematic illustration of procedure for preparing the LBL-assembled multilayer-coated spheres consisting of titania nanosheets and GO nanosheets, followed by microwave reduction of GO into G. Reproduced with permission.[77] Copyright 2012, Wiley-VCH.

method, in which TiO_2 first grew on GO sheets by hydrolysis of $Ti(BuO)_4$ and then crystallized into anatase nanocrystals by hydrothermal treatment.[78] The density of TiO_2 nanocrystals on graphene could be controlled by feed ratio of $Ti(BuO)_4$/GO. TiO_2–graphene composites was also prepared with in situ growth of TiO_2 in the interlayer of inexpensive expanded graphite under ethanol-assisted solvothermal conditions,[79] in which graphene possesses few defects and high-quality electrical properties for excellent photocatalytic efficiency.[55] A in situ simultaneous reduction-hydrolysis technique (SRH) was exploited to fabricate 2D sandwich-like graphene-TiO_2 hybrid nanosheets in a binary ethylenediamine (En)/H_2O solvent.[80] The so-called SRH technique is based on the mechanism of the simultaneous reduction of GO into graphene by En and the formation of TiO_2 nanoparticles through hydrolysis of titanium (IV) (ammonium lactato) dihydroxybis, subsequently in situ loading onto graphene through chemical bonds (Ti-O-C bond) to form 2D sandwich-like nanostructure. On the one hand, graphene serves as a two-dimensional "mat" well to anchor the forming TiO_2 nanoparticles to restrain from growing into large particles; on the other hand, the dispersion of TiO_2 hinders the collapse and restacking of exfoliated sheets of graphene during reduction process. High-quality nano-sized anatase ultrathin TiO_2 nanosheets mainly dominated by {001} facets were grown on graphene nanosheets by a simple one-pot solvothermal synthetic route.[81,82]

Graphene-CdS quantum dots nanocomposites was prepared by mixing GO and $Cd(CH_3COO)_2$ in dimethyl sulfoxide (DMSO) and then heating in an autoclave, which guaranteed that the reduction of GO and the deposition of CdS on graphene occurred simultaneously.[51,83] During the synthetic process, DMSO served as both a solvent and a source of sulfur. In situ growth was also used to grow other oxides and hydroxides on graphene, including Bi_2WO_6,[84] ferrite (MFe_2O_4, M = Mn, Zn, Co and Ni),[69,85–89] $Mg(OH)_2$,[90] and BiOBr.[91–93] Graphene-$CoFe_2O_4$ photocatalsyts with different content of graphene were prepared by mixing of GO, $Co(NO_3)_2$ and $Fe(NO_3)_3 \cdot 9H_2O$ in ethanol solution followed by hydrothermal treatment.[86]

4. Application of Graphene-Based Photocatalysts

Graphene-based photocatalysts have been widely applied in the following fields as shown in **Figure 5** and listed in Table 1:

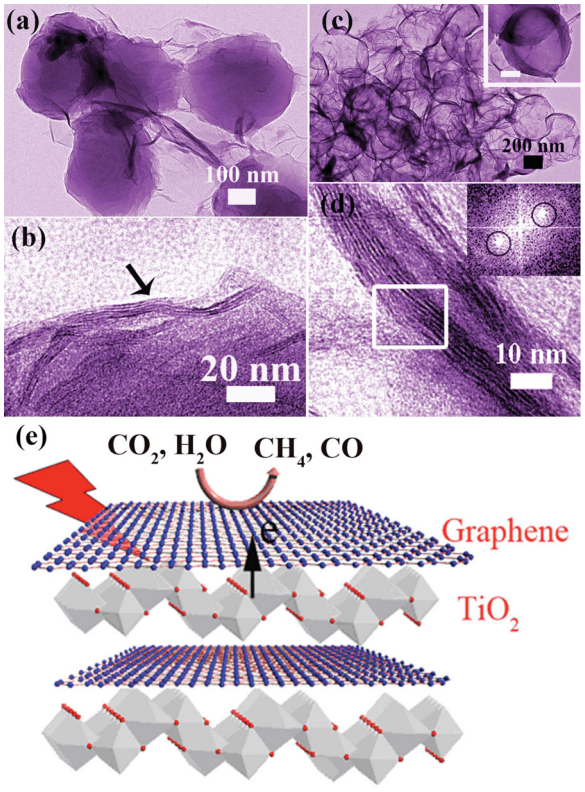

Figure 4. TEM images of a,b) PMMA spheres coated with $(PEI/Ti_{0.9}O_2/PEI/GO)_5$, c,d) $(G\text{-}Ti_{0.9}O_2)_5$ hollow spheres, e) atomistic model for the selected area in (d). Reproduced with permission.[77] Copyright 2012, Wiley-VCH.

(1) water splitting; (2) degradation or oxidization of organic contaminants; (3) photocatalytic conversion of CO_2 to renewable fuels; (4) toxic elimination of heavy metal ions and antibacterial applications.

4.1. Photocatalytic Water Splitting

Harvesting solar energy to split water is one of the cleanest ways to produce H_2 and O_2, which has great potential in increasing demand for energy and associated environmental problems, because producing H_2 from water using solar energy is a promising solution to develop a carbon-free fuel and sustainable energy system. However, the practical applications of this technique are limited by the inability to utilize visible light, insufficient quantum efficiency, and/or photo-degradation of the catalyst.[94] Design of novel catalysts to meet the industrial needs is still a challenge.

GO with different oxygenated levels showed potential as a photocatalyst for H_2 and O_2 evolution from water with the presence of sacrificial reagents.[95,96] Considering the superior electron mobility and high specific surface area, graphene also shows more promising as an efficient electron acceptor to enhance the photoinduced charge transfer and inhibit the backward reaction by separating the evolution sites of hydrogen and oxygen for improving photocatalytic H_2-production activity

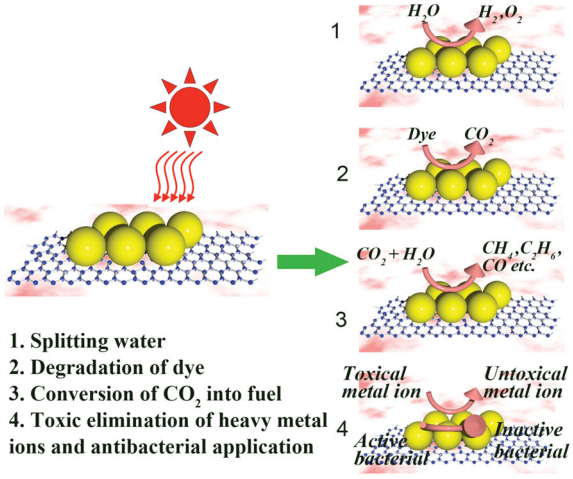

Figure 5. Various applications of graphene-based photocatalysts.

(**Figure 6**). TiO_2-5 wt% graphene composites by sol–gel method showed about 2-time enhancement for H_2 evolution than P25 (H_2: 4.5 μmol h^{-1}) under UV-vis illumination, which was proposed to the reduction of electron-hole recombination with the introduction of graphene.[97] P25-RGO composites prepared with several techniques including UV-assisted photocatalytic reduction, hydrazine reduction, and hydrothermal method exhibited significantly higher rates of H_2 evolution than that for P25 alone under UV-vis irradiation,[98] among which one prepared by the hydrothermal method (mass ratio of P25/RGO = 1/0.2, H_2: 74 μmol h^{-1}) exhibited the best performance, showing 1 order of magnitude higher than that for P25 alone (H_2: 6.8 μmol h^{-1}), due to that stronger interaction between P25 and graphene caused by the hydrothermal method. Such P25-RGO composite was also more effective than P25-carbon nanotubes composite for H_2 evolution. Theoretical calculations reveal that the {001} facets of anatase TiO_2 are the most reactive facets with a high surface energy.[99,100] Graphene-modified TiO_2 nanosheets with exposed {001} facets (the graphene content is 1 wt%, H_2: 736 μmol h^{-1}, the quantum efficiency is 3.1%,) showed over 41-times enhancement for H_2 evolution than that of pure TiO_2 nanosheets (H_2: 18 μmol h^{-1}) under UV-vis irradiation.[101] A distinct high quantum efficiency of 9.7% at 365 nm (H_2: 165.3 μmol h^{-1}) was achieved by TiO_2/MoS_2/graphene composites with the content of the MoS_2/graphene co-catalyst of 0.5 wt% and the content of graphene in this co-catalyst of 5.0 wt%.[102] This unusual photocatalytic activity arises from the

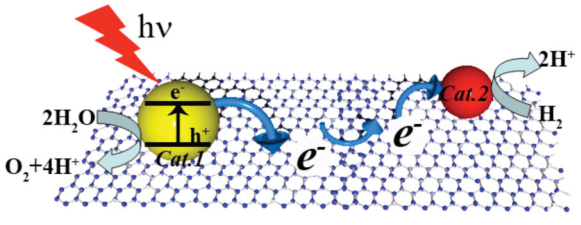

Figure 6. Schematic illustration of selective catalysis of water splitting at different sites on graphene used as a conducting support.

positive synergetic effect between the MoS_2 and graphene components in this hybrid co-catalyst, which serve as an electron collector and a source of active adsorption sites, respectively.

CdS is one of the most studied visible-light-driven photocatalysts because of its relatively narrow band gap (2.4 eV). However, it suffers from the low separation efficiency of electron–hole pairs and photocorrosion during light irradiation.[47,48] Graphene-decorated with CdS clusters with 1.0 wt% graphene and 0.5 wt% Pt showed a apparent quantum effciency of 22.5% (λ = 420 nm) and the H_2-production rate of 1.12 mmol h^{-1} (about 4.87 times higher than that of pure CdS nanoparticles with 0.5 wt% Pt).[62] N-graphene/CdS nanocomposites exhibited remarkable photocatalytic ability for the continuous and stable production of H_2 from water under visible light irradiation at $\lambda > 420$ nm with H_2 evolution rate of 210 μmol h^{-1} (the graphene content is 2 wt%), 5 times higher than that of pure CdS (40 μmol h^{-1}).[103] N-graphene as a co-catalyst can also prevent CdS from photocorrosion under light irradiation, resulting in no deactivation for H_2 evolution for longer than 30 h. The rapid and favorable transferring of electrons from CdS to graphene and high separation effciency of electron-hole pairs led to the dramatic enhancement of photoactivity and complete inhibition of photocorrosion, due to the excellent conductivity of N-graphene. CdS-sensitized TaON core–shell composites coupled with 1 wt% GO and 0.4 wt% Pt exhibited high H_2-production rate of 633 μmol h^{-1} under visible light and a apparent quantum efficiency of 31% at 420 nm,[104] and the rate of H_2 formation was about 2 times and 141 times higher than that of CdS@TaON core–shell composites and the pristine TaON, respectively. This high activity was ascribed to the presence of CdS nanocrystals that form a heterojunction with TaON and the involvement of GO that serves as an electron collector and transporter to efficiently lengthen the lifetime of the photogenerated charge carriers.

Other graphene-based photocatalysts such as g-C_3N_4-graphene,[66] graphene-$Sr_2Ta_2O_{7-x}N_x$,[105] graphene-$Zn_xCd_{1-x}S$,[106] and graphene-Cu_2O[107] were also synthesized to efficiently produce H_2 from water. g-C_3N_4 as a metal-free polymeric photocatalyst is considered as a promising visible-driven photocatalyst. g-C_3N_4 with 1 wt% graphene and 1.5 wt% Pt co-catalyst showed H_2-production rate of 451 μmol h^{-1} g^{-1} and a quantum efficiency of 2.6% under visible-light irradiation (>400 nm), and the H_2-production rate was more 3-times than pure g-C_3N_4 with 1.5 wt% Pt co-catalyst.[66] Z-scheme photocatalytic system, as a multi-photon water splitting system, consists of a H_2-evolution photocatalyst, O_2-evolution photocatalyst, and a reversible electron mediator, which achieves a dynamic equilibrium between the electron-accepting and -donating abilities. Graphene was proved to act as a promising solid electron mediator for water splitting in the Z-scheme photocatalysis system (**Figure 7**).[108] Graphene can shuttle photogenerated electrons from a O_2-evolution photocatalyst ($BiVO_4$) to a H_2-evolution photocatalyst (Ru/$SrTiO_3$:Rh), tripling the consumption of electron-hole pairs in the water splitting reaction under visible-light irradiation. The key factor that enables for effcient electron transfer in a Z-scheme system lies in achieving a balance between the degree of GO reduction (for conductivity restoration) and the level of hydrophobicity of graphene. It should be noted that while a suitable content of graphene is crucial for optimizing

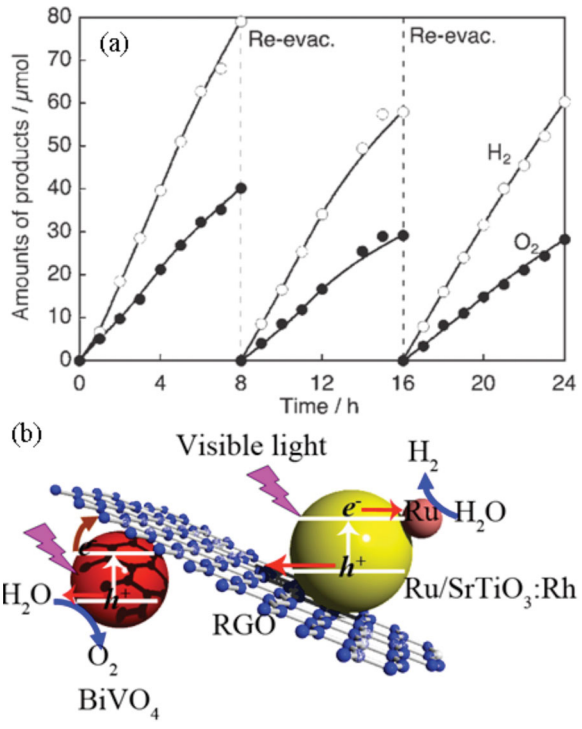

Figure 7. a) Overall water splitting under visible-light irradiation by the ($Ru/SrTiO_3$:Rh and $RGO/BiVO_4$ system. The activity during the second cycle was slightly decreased, as is normally observed for most systems, and the activity at third cycle was almost the same as that of the second cycle, implying a stable system after the second cycle. Reproduced with permission.[108] Copyright 2011, American Chemical Society. b) Mechanism of water splitting in a Z-scheme photocatalysis system consisting of $Ru/SrTiO_3$:Rh and $RGO/BiVO_4$ under visible-light irradiation.

the photocatalytic activity of graphene-based nanocomposites, the excessive incorporation of graphene may diminish the photocatalytic activity.[62,66] The reason is that a large percentage of graphene shields the active sites on the catalyst surface and also rapidly decreases the intensity of light through the depth of reactants, which could be called a "shielding effect".

4.2. Photocatalytic Degradation or Oxidization of Organic Contaminants

Graphene-based photocatalysts also exhibit great potential for photocatalytic degradation or oxidization organic contaminants such as methylene blue (MB), methyl orange (MO), rhodamine B (RhB), phenol, butane and 2-propanol.[54,60,61,69–76,79,80,83–87,90,91,109–169] Generally, the photocatalytic degradation or oxidization of organic contaminants depends on the generation of the oxygen species especially •OH radicals, which can subsequently oxidize the organic contaminants. The fundamental mechanism of graphene-based photocatalysts for degradation or oxidization of organic contaminants was proposed to be similar with the case over the other carbon (such as carbon nanotubes and activated carbon)-based photocatalysts.[70,72,170–172] The electron from semiconductor nanoparticles can transport along the GO sheets and then react with the absorbed O_2 to form $\cdot OH$ for the further photocatalytic degradation of pollutants.[72] Due to the hindrance of the electron-hole recombination caused by the effective charge transfer between graphene and semiconductors, the production of $\cdot OH$ and $\cdot O_2^-$ species under the light irradiation can increase, which could be confirmed from the intensity of $\cdot OH$ and $\cdot O_2^-$ species with the assist of ESR spectra.[53,107] Therefore, the increase of $\cdot OH$ and $\cdot O_2^-$ species leads to the higher photocatalytic efficiency of graphene-based photocatalysts.

Much works have been made in the investigation of graphene-shape controlled TiO_2 photocatalysts for the degradation or oxidation of organic contaminants, including particles,[61,70,73,79,117,132,135,137] nanorods,[72,121,173] nanotubes,[120,129,159,160] nanoplates,[76] nanospheres,[60] one-dimensional rice-shaped mesostructure,[168] and {001} facets-exposed nanocrystalline TiO_2.[116,151,161] P25-graphene composite showed higher photocatalytic activity for the photodegradation of MB than that of bare P25 under UV light, which was ascribed to the enhanced adsorptivity of dyes and the suppression of the electron–hole recombination.[61] The enhanced adsorption of MB originates from abundant π–π conjugations between MB molecules and the aromatic rings of graphene nanosheets, rather than simple physical adsorption, evidenced by no significant changes in the BET specific area.[61] The graphene-TiO_2 nanotubes composites with 10 wt% graphene illustrated a 3-fold enhancement in photocatalytic effciency over pure TiO_2 nanotubes in a quartz reactor.[159] A strongly electronic-coupled nanocomposites of lepidocrocite-type layered titanate and graphene nanosheets showed a higher activity for the photodegradation of organic molecules than uncomposited layered titanate under UV–vis illumination (λ > 300 nm).[76] Ultrathin TiO_2 nanosheets mainly dominated by {001} facets-graphene composites exhibited a much high photocatalytic degradation of organic contaminants compared with the pure TiO_2 nanosheet and commercial P25 due to the most reactive facets of the {001} facets with a high surface energy and the effective separation of photogenerated charge based on the electron transfer from TiO_2 to graphene.[82,116,151,161]

The hybrid of graphene and semiconductors can increase the absorption of light intensity and extend the light absorption range, so more efficient utilization of the solar energy is obtained. Typically, graphene-TiO_2 nanoparticle composites usually exhibit a red shift of the band-edge and a significant reduction of the bandgap, which may be caused by the interaction between unpaired π electrons of graphene and Ti atoms[60] and the chemical bonding (Ti-O-C bond) between TiO_2 and graphene.[61] The visible light photoactivity of graphene-based photocatalyst is promising to facilitate its use in practical environmental remediation for photocatalytic degradation or oxidation of organic contaminants. Graphene-TiO_2 nanocomposites was proved for photocatalytic degradation or oxidation of organic contaminants under visible light caused by the incorporation of graphene or GO, including MB,[60,70,71,73,135,137,145,151] benzyl alcohol,[134] RhB,[124,158,161] butane,[123] and MO.[168] P25-graphene composite displayed remarkable improvement for the photodegradation of MB molecules under visible light irradiation (λ > 400 nm) compared to P25,[61] because an obvious red shift of ca. 30–40 nm in the absorption edge of

P25-graphene powder, compared to bare P25. Wrapping of TiO_2 nanoparticles with graphene nanosheets highly enhanced the photocatalytic activity of TiO_2 for the photodegradation of MB under visible light irradiation ($\lambda > 420$ nm) compared to pure TiO_2 nanoparticles and P25, which is attributed to bandgap narrowing (3.2 eV $\rightarrow$ 2.8 eV) of TiO_2 in the graphene-TiO_2 nanocomposties and allows more absorption of visible light.[60] The composites of Fe-doped TiO_2 (Fe/Ti ratio: 0.5 at%) and graphene showed superior photocatalytic activity than graphene-TiO_2 under visible irradiation ($\lambda > 420$ nm) for MO degradation. The enhanced photocatalytic activity may be attributed to the synergistic effect of enhanced visible light absorption caused by the incorporation of graphene and Fe ion, improved adsorptivity of dyes, and effective charge separation. CdS-TiO_2-graphene composites possessed a maximum degradation efficiency of 99.5% for photocatalytic degradation of MO under visible light irradiation ($\lambda > 400$ nm) compared with the pure TiO_2 (43%) and CdS–TiO_2 (79.9%) composites.[154] CdS–graphene–TiO_2 hybrids also display enhanced photocatalytic activity for selective oxidation of alcohols to aldehydes under visible-light irradiation ($\lambda > 420$ nm) compared with CdS-graphene composites, which was ascribed to the combined interaction the longer lifetime of photogenerated electron-hole pairs, faster interfacial charge-transfer rate, and larger surface area.[174] ZnS-RGO nanocomposites exhibited visible light photoactivity toward aerobic selective oxidation of alcohols and epoxidation of alkenes under ambient conditions, due to that the role of RGO in the ZnS-RGO nanocomposites acts as an organic dye-like macromolecular "photosensitizer" for ZnS instead of an electron reservoir.[175] Ag_3PO_4 as a new visible light photocatalyst for the oxidation of water and photodecomposition of organic compounds is unstable upon photo-illumination, which is easy to be corroded by the photogenerated electrons ($4Ag_3PO_4 + 6H_2O + 12h^+ + 12e^- \rightarrow 12Ag + 4H_3PO_4 + 3O_2$).[176,177] Incorporation of GO with Ag_3PO_4 not only improves photocatalytic activity for the degradation of organic dyes (AO7 and phenol) under visible-light irradiation (630 nm > λ > 420 nm), compared with bare Ag_3PO_4,[178], but also the stability of Ag_3PO_4 was much enhanced during photocatalytic process.[178,179]

Polymeric g-C_3N_4 is a promising photocatalyst for contaminant removal under visible light irradiation.[180] However, the low quantum efficiency for this pristine semiconductor limited its photocatalytic performance. GO modified g-C_3N_4 fabricated by sonochemical approach showed remarkable improvement for photocatalytic degradation of RhB and 2, 4-dichlorophenol under visible light irradiation ($\lambda > 400$ nm), which was 3.80 and 2.08 times in the photodegradation rate than that of pristine g-C_3N_4, respectively.[150] This enhanced photocatalytic activity resulted from the effective photogenerated charge separation efficiency owing to the heterojunction building between GO and g-C_3N_4. Graphene-Ferrites (MFe_2O_4, M = Mn, Zn, Co and Ni)[69,85–87] composites have been used to remove pollutants in water, because it is convenient to recover and reuse suspended nanosized photocatalysts through magnetic separation from suspension system after degradation.

Plasmon-mediated photocatalysis recently becomes a rising research star in the harvesting and conversion of solar energy (especially in visible region), because photocatalysts containing semiconductors and plasmonic nanostructures of noble metals (mainly silver and gold) can enhance the photocatalytic activity primarily by extending the optical absorption to the visible light region and enhancing the concentration of charge carriers through an excitation of surface plasmon resonance (SPR).[181] Ag/anatase TiO_2/graphene composite, as a visible light-activated photocatalyst, exhibited significantly increased visible light absorption and improved photocatalytic activity for the degradation of MB under visible light ($\lambda > 410$ nm) compared with Ag/TiO_2 and TiO_2/graphene nanocomposites.[125] The increased absorption in visible light region was originated from the strong interaction between TiO_2 nanoparticles and graphene, as well as SPR effect of Ag nanoparticles that are mainly adsorbed on the surface of TiO_2 nanoparticles. Ag/AgCl/GO[74] and Ag/AgBr/GO[74,75] nanocomposites fabricated via a water/oil or oil/water system were also used as stable plasmonic photocatalysts for the photodegradation of MO pollutant under visible light irradiation. A Ag-ZnO-graphene multidimensional heterojunction composed of a zero-dimensional Ag nanoparticle, one-dimensional ZnO nanorods, and two-dimensional graphene improved photocatalytic activity by increasing light absorption, preventing photo-induced electron–hole recombination, and providing a carrier pathway for the giant π-conjugated system of graphene.[165]

4.3. Photocatalytic Conversion of CO_2 to Renewable Fuels

CO_2 is a greenhouse gas of growing concern, and its atmospheric concentration continues to rise from the ongoing burning of fossil fuels. The idea of mimicking the overall natural photosynthetic cycle of the chemical conversion of CO_2 into useful fuels has been consistently gaining attention for more than 30 years.[46,182,183] Photocatalytic conversion of CO_2 to valuable hydrocarbons using solar energy is one of the best solutions to both the global warming and the energy shortage problems.

Among the present photocatalysts for the CO_2 photoconversion, TiO_2-based semiconductor photocatalysts have been considered the most popular and efficient. The combination of graphene proves an promising way to further improve photocatalytic activity of TiO_2.[55,77,80,184] Robust hollow spheres consisting of molecular-scale $Ti_{0.91}O_2$ nanosheets and graphene nanosheets as building blocks were fabricated for photocatalytic CO_2 conversion into renewable fuel.[77] The 9-time significant increase of photocatalytic activity of graphene-$Ti_{0.91}O_2$ hollow spheres was confirmed with photoreduction of CO_2 into renewable fuels (dominant CO and minor CH_4), relative to commercial P25. The large enhancement of the photocatalytic activity benefits from: (1) the ultrathin nature of $Ti_{0.91}O_2$ nanosheets allows charge carriers to move rapidly onto the surface to participate in the photoreduction reaction; (2) The sufficiently compact stacking of ultrathin $Ti_{0.91}O_2$ nanosheets with graphene nanosheets allows the photogenerated electron to fast transfer from $Ti_{0.91}O_2$ nanosheets to G to enhance lifetime of the charge carriers; (3) The hollow structure potentially acts as a photon trap well to allow the multi-scattering of incidence light for the enhancement of light absorption. The possible reason for dominant production of CO over CH_4 may be explained as following: the transferred electrons to graphene

diffuse quickly on a larger area of graphene, befitting from the enhanced electrical mobility of graphene. It restrains the accumulation of the electrons and decrease local electron density, which is favorable for two-electron interaction to form CO. In contrast with prevenient graphene-TiO_2 nanocomposites, the graphene-TiO_2 hybrid prepared with the SRH route (mentioned in *in* situ growth of Part 3) shows high and selective photocatalytic activity toward conversion of CO_2 to CH_4 and C_2H_6 in the presence of water vapor[80] (**Figure 8**). The synergistic effect of the surface-Ti^{3+} sites through reduction of Ti^{4+} caused by reducing agent En and graphene favors the generation of C_2H_6, and the yield of the C_2H_6 increased with the content of incorporated graphene. The existence of abundance of Ti^{3+} sites favors the coupling of photo-formed $\cdot CH_3$ radicals into C_2H_6 compared with commercial P25 and graphene-P25, which only produce CH_4. $\cdot CH_3$ radicals may also be absorbed on the surface of graphene via π-conjugation between the unpaired electron of the radical and aromatic regions of the graphene.[61,72]

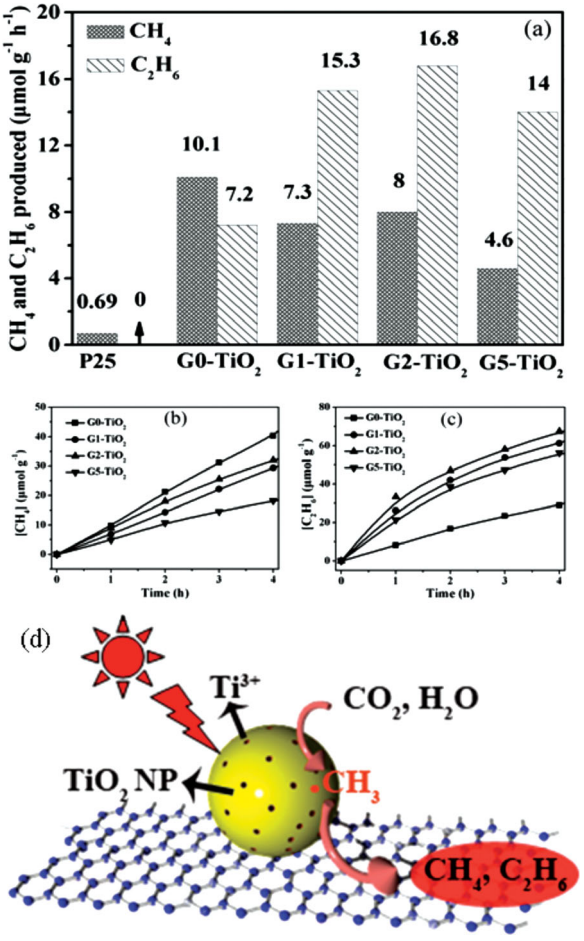

Figure 8. a) Comparison of photocatalytic activity of samples G*x*-TiO_2 (*x* = 0, 1, 2, 5) and P25. The molar ratio of C_2H_6 to CH_4 increases from 0.71 (for G0-TiO_2), 2.09 (G1-TiO_2), 2.10 (G2-TiO_2), to 3.04 (G5-TiO_2). b,c) Photocatalytic CH_4 and C_2H_6 evolution amounts for samples G*x*-TiO_2 (*x* = 0, 1, 2, 5). Reproduced with permission.[80] Copyright 2012, Wiley-VCH. d) Schematic illustration of photocatalytic conversion of CO_2 into CH_4 and C_2H_6 over TiO_2-graphene hybrid nanosheets prepared by SRH technique.

The electron-rich graphene may help stabilize the $\cdot CH_3$ species, which restrains combination of $\cdot CH_3$ with H^+ and e^{-1} into CH_4. Meanwhile, subsequent increasing accumulation of $\cdot CH_3$ on the graphene raises the opportunity of formation of C_2H_6 by the coupling of $\cdot CH_3$. This work may open a new doorway for new significant application of graphene for selectively catalytic C-C coupling reaction. Compared to methods powered by thermal energy, techniques that use photonic energy to directly drive C-C coupling of CO_2 at room temperature undoubtedly have substantial advantages, such as the capacity to minimize coking.[185]

The influence of the different defect densities of graphene on the photocatalystic reduction of CO_2 to CH_4 was investigated by preparing graphene-P25 nanocomposite thin films through two major solution-based pathways, oxidation reduction and solvent exfoliation.[55] The optimized graphene-P25 nanocomposites based on the less defective solvent-exfoliated graphene yield approximately 7-fold improvements in the photoreduction of CO_2, compared to P25 alone under visible illumination. The improved electrical mobility of the less defective graphene allows photoexcited electrons to more effectively diffuse to reactive sites, facilitating photoreduction reactions.

4.4. Toxic Elimination of Heavy Metal Ions and Antibacterial Applications

The presence of toxic metal ions in aquatic bodies has been known to cause pollution problems, which may be a health hazard to both humans and animals. Toxicity of metal ions can be eliminated through photocatalytic reduction into innoxious analogue ions using solar energy, such as Cr(VI) into Cr(III). Graphene-based photocatalysts prove great potential for efficiency enhancement of photoreduction of toxic metal ions.[117,186–188] CdS–RGO composites enhanced photocatalytic performance for the reduction of Cr(VI) with a maximum removal rate of 92% under visible light irradiation as compared with pure CdS (79%) due to the increased light absorption intensity and the reduction of electron–hole pair recombination in CdS with the introduction of RGO.[188] ZnO–graphene composites exhibited the photocatalytic reduction of Cr(VI) with a maximum removal rate of 98% under UV light irradiation as compared with pure ZnO (58%).[186] TiO_2 nanoparticles assembled on GO nanosheets show 5.4-time increase of photocatalytic activity for reduction of Cr(VI), relative to commercial P25.[117]

Graphene-based photocatalysts have also been employed for antibacterial applications.[189–191] Akhavan et al.[189] investigated the effect of graphene on photoinactivation of bacteria by testing the antibacterial activity of the graphene/TiO_2 thin films against E. coli bacteria under solar light irradiation. The detected highest antibacterial activity was achieved by graphene/TiO_2 thin film after UV exposure for 4 h, with 7.5 times relative to the bare TiO_2 thin film. The mechanism of GO/TiO_2 hybrid-mediated photodynamic cancer cell death originates from that the reactive oxygen species (ROSs) such as hydrogen peroxide (H_2O_2), •OH, and $\cdot O_2^-$ were formed under UV light exposure of TiO_2.[191] Such ROSs react with cell membranes and the cell interior, and affect cell rigidity and chemical arrangement of surface structures, leading to cell toxicity. The

ROS accumulation produced by GO/TiO_2 hybrid at 100 μg/mL increased 5.32 times than that of pure TiO_2 under visible light irradiation.

5. Conclusions and Outlook

This Feature Article demonstrates a clear phenomenon that graphene-based photocatalysts represent a new class of promising materials in the field of photo-driven chemical conversion using abundant solar energy in water splitting, degradation or oxidization of organic contaminants, conversion of CO_2 into renewable fuels, photoreduction of toxic metal ions, and antibacterial applications. The photocatalytic enhancement of graphene-based nanocomposites is caused by the reduction of the recombination of electron-hole pairs, the extension of the light absorption range, increased absorption of light intensity, more surface active sites, and improvement of chemical stability of photocatalysts. Production of graphene in large quantities and at a low cost offers the hybrid photocatalysts tremendous opportunities for practical application. The principal challenge to facilitate the development of graphene-based photocatalysts lies in understanding reciprocity of graphene and semiconductor after hybridation, including rearrangement and couple of energy band structures and graphene-promoting enhancement of chemical stability of photocatalysts.

Acknowledgements

This work was supported by 973 Programs (No. 2011CB933303, 2013CB632404), Natural Science Foundation of Jiangsu Province (No. BK2012015), Fundamental Research Funds for the Central Universities (No. 1113020401, 1115020405 and 1116020406), and NSFC (No. 20971048).

Received: December 1, 2012
Revised: January 7, 2013
Published online: May 5, 2013

[1] K. S. Novoselov, A. K. Geim, S. V. Morozov, D. Jiang, Y. Zhang, S. V. Dubonos, I. V. Grigorieva, A. A. Firsov, *Science* **2004**, *306*, 666.
[2] K. S. Novoselov, A. K. Geim, S. V. Morozov, D. Jiang, M. I. Katsnelson, I. V. Grigorieva, S. V. Dubonos, A. A. Firsov, *Nature* **2005**, *438*, 197.
[3] Y. Zhang, Y. W. Tan, H. L. Stormer, P. Kim, *Nature* **2005**, *438*, 201.
[4] A. K. Geim, K. S. Novoselov, *Nat. Mater.* **2007**, *6*, 183.
[5] K. I. Bolotin, K. J. Sikes, Z. Jiang, M. Klima, G. Fudenberg, J. Hone, P. Kim, H. L. Stormer, *Solid. State. Commun.* **2008**, 146, 351.
[6] M. J. Allen, V. C. Tung, R. B. Kaner, *Chem. Rev.* **2009**, *110*, 132.
[7] C. Lee, X. Wei, J. W. Kysar, J. Hone, *Science* **2008**, *321*, 385.
[8] M. D. Stoller, S. Park, Y. Zhu, J. An, R. S. Ruoff, *Nano Lett.* **2008**, *8*, 3498.
[9] R. R. Nair, P. Blake, A. N. Grigorenko, K. S. Novoselov, T. J. Booth, T. Stauber, N. M. R. Peres, A. K. Geim, *Science* **2008**, *320*, 1308.
[10] A. A. Balandin, S. Ghosh, W. Bao, I. Calizo, D. Teweldebrhan, F. Miao, C. N. Lau, *Nano Lett.* **2008**, *8*, 902.
[11] S. Ghosh, I. Calizo, D. Teweldebrhan, E. P. Pokatilov, D. L. Nika, A. A. Balandin, W. Bao, F. Miao, C. N. Lau, *Appl. Phys. Lett.* **2008**, *92*, 151911.
[12] P. R. Somani, S. P. Somani, M. Umeno, *Chem. Phys. Lett.* **2006**, *430*, 56.
[13] S. J. Park, R. S. Ruoff, *Nat. Nanotechnol.* **2009**, *4*, 217.
[14] K. S. Kim, Y. Zhao, H. Jang, S. Y. Lee, J. M. Kim, K. S. Kim, J. H. Ahn, P. Kim, J. Y. Choi, B. H. Hong, *Nature* **2009**, *457*, 706.
[15] X. Li, W. Cai, J. An, S. Kim, J. Nah, D. Yang, R. Piner, A. Velamakanni, I. Jung, E. Tutuc, S. K. Banerjee, L. Colombo, R. S. Ruoff, *Science* **2009**, *324*, 1312.
[16] A. Malesevic, R. Vitchev, K. Schouteden, A. Volodin, L. Zhang, G. Van Tendeloo, A. Vanhulsel, C. Van Haesendonck, *Nanotechnology* **2008**, 19.
[17] X. Yang, X. Dou, A. Rouhanipour, L. Zhi, H. J. Räder, K. Müllen, *J. Am. Chem. Soc.* **2008**, *130*, 4216.
[18] C. H. Lu, H. H. Yang, C. L. Zhu, X. Chen, G. N. Chen, *Angew. Chem. Int. Ed.* **2009**, *48*, 4785.
[19] X. Yan, X. Cui, L. S. Li, *J. Am. Chem. Soc.* **2010**, *132*, 5944.
[20] Z. P. Chen, W. C. Ren, L. B. Gao, B. L. Liu, S. F. Pei, H. M. Cheng, *Nat. Mater.* **2011**, *10*, 424.
[21] Y. Hernandez, V. Nicolosi, M. Lotya, F. M. Blighe, Z. Y. Sun, S. De, I. T. McGovern, B. Holland, M. Byrne, Y. K. Gun'ko, J. J. Boland, P. Niraj, G. Duesberg, S. Krishnamurthy, R. Goodhue, J. Hutchison, V. Scardaci, A. C. Ferrari, J. N. Coleman, *Nat. Nanotechnol.* **2008**, *3*, 563.
[22] X. Li, G. Zhang, X. Bai, X. Sun, X. Wang, E. Wang, H. Dai, *Nat. Nanotechnol.* **2008**, *3*, 538.
[23] J. Z. Wang, K. K. Manga, Q. L. Bao, K. P. Loh, *J. Am. Chem. Soc.* **2011**, *133*, 8888.
[24] X. L. Li, X. R. Wang, L. Zhang, S. W. Lee, H. J. Dai, *Science* **2008**, *319*, 1229.
[25] D. V. Kosynkin, A. L. Higginbotham, A. Sinitskii, J. R. Lomeda, A. Dimiev, B. K. Price, J. M. Tour, *Nature* **2009**, *458*, 872.
[26] L. Jiao, X. Wang, G. Diankov, H. Wang, H. Dai, *Nat. Nanotechnol.* **2010**, *5*, 321.
[27] a) L. J. Cote, F. Kim, J. Huang, *J. Am. Chem. Soc.* **2009**, *131*, 1043; b) K. P. Loh, Q. L. Bao, P. K. Ang, J. X. Yang, *J. Mater. Chem.* **2010**, *20*, 2277.
[28] W. S. Hummers, R. E. Offeman, *J. Am. Chem. Soc.* **1958**, *80*, 1339.
[29] S. Myung, J. Park, H. Lee, K. S. Kim, S. Hong, *Adv. Mater.* **2010**, *22*, 2045.
[30] X. Wang, L. Zhi, K. Mullen, *Nano Lett.* **2007**, *8*, 323.
[31] Q. He, H. G. Sudibya, Z. Yin, S. Wu, H. Li, F. Boey, W. Huang, P. Chen, H. Zhang, *ACS Nano* **2010**, *4*, 3201.
[32] Y. Zhou, Q. L. Bao, B. Varghese, L. A. L. Tang, C. K. Tan, C. H. Sow, K. P. Loh, *Adv. Mater.* **2010**, *22*, 67.
[33] S. B. Yang, X. L. Feng, K. Mullen, *Adv. Mater.* **2011**, *23*, 3575.
[34] N. L. Yang, J. Zhai, D. Wang, Y. S. Chen, L. Jiang, *ACS Nano* **2010**, *4*, 887.
[35] a) Q. L. Bao, H. Zhang, Y. Wang, Z. H. Ni, Y. L. Yan, Z. X. Shen, K. P. Loh, D. Y. Tang, *Adv. Funct. Mater.* **2009**, *19*, 3077; b) Q. L. Bao, H. Zhang, J. X. Yang, S. Wang, D. Y. Tong, R. Jose, S. Ramakrishna, C. T. Lim, K. P. Loh, *Adv. Funct. Mater.* **2010**, *20*, 782; c) Q. L. Bao, H. Zhang, B. Wang, Z. H. Ni, C. H. Y. X. Lim, Y. Wang, D. Y. Tang, K. P. Loh, *Nat. Photonics* **2011**, *5*, 411.
[36] S. W. Hwang, D. H. Shin, C. O. Kim, S. H. Hong, M. C. Kim, J. Kim, K. Y. Lim, S. Kim, S. H. Choi, K. J. Ahn, G. Kim, S. H. Sim, B. H. Hong, *Phys. Rev. Lett.* **2010**, 105.
[37] a) X. Huang, Z. Yin, S. Wu, X. Qi, Q. He, Q. Zhang, Q. Yan, F. Boey, H. Zhang, *Small* **2011**, *7*, 1876; b) Y. Zhu, D. K. James, J. M. Tour, *Adv. Mater.* **2012**, *24*, 4924; c) D. Zhan, J. X. Yan, L. F. Lai, Z. H. Ni, L. Liu, Z. X. Shen, *Adv. Mater.* **2012**, *24*, 4055.
[38] a) T. Gan, S. S. Hu, *Microchim. Acta.* **2011**, *175*, 1; b) Dale A. C. Brownson, D. K. Kampouris, C. E. Banks, *Chem. Soc. Rev.* **2012**, *41*, 6944; c) D. Q. Wu, F. Zhang, H. W. Liang, X. L. Feng, *Chem. Soc. Rev.* **2012**, *41*, 6160; d) Y. H. Ng, S. Ikeda, M. Matsumura, R. Amal, *Energy Environ. Sci.* **2012**, *5*, 9307.
[39] a) S. J. Guo, S. J. Dong, *J. Mater. Chem.* **2011**, *21*, 18503; b) X. J. Wan, Y. Huang, Y. S. Chen, *Accout. Chem. Res.* **2012**, *45*,

598; c) H. X. Chang, H. K. Wu, *Adv. Funct. Mater.* **2012**, *23*, 1984; d) Y. X. Liu, X. C. Dong, P. Chen, *Chem. Soc. Rev.* **2012**, *41*, 2283.
[40] a) Y. Zhou, K. P. Loh, *Adv. Mater.* **2010**, *22*, 3615; b) Q. L. Bao, K. P. Loh, *ACS Nano* **2012**, *6*, 3677.
[41] a) D. A. C. Brownson, D. K. Kampouris, C. E. Banks, *J. Power. Sources* **2011**, *196*, 4873; b) K. S. Novoselov, V. I. Fal'ko, L. Colombo, P. R. Gellert, M. G. Schwab, K. Kim, *Nature* **2012**, *490*, 192; c) X. Huang, X. Y. Qi, F. Boey, H. Zhang, *Chem. Soc. Rev.* **2012**, *41*, 666; d) Y. Chen, B. Zhang, G. Liu, X. Zhuang, E. T. Kang, *Chem. Soc. Rev.* **2012**, *41*, 4688.
[42] a) B. Luo, S. Liu, L. Zhi, *Small* **2012**, *8*, 630; b) P. V. Kamat, *J. Phys. Chem. Lett.* **2010**, *1*, 520.
[43] a) M. Pumera, *Energ. Environ. Sci.* **2011**, *4*, 668; b) C. C. Huang, C. Li, G. Q. Shi, *Energ. Environ. Sci.* **2012**, *5*, 8848.
[44] Y. Q. Sun, Q. O. Wu, G. Q. Shi, *Energ. Environ. Sci.* **2011**, *4*, 1113.
[45] a) Y. H. Hu, H. Wang, B. Hu, *ChemSusChem* **2010**, *3*, 782; b) M. Pumera, *Chem. Soc. Rev.* **2010**, *39*, 4146.
[46] T. Inoue, A. Fujishima, S. Konishi, K. Honda, *Nature* **1979**, *277*, 637.
[47] J. F. Reber, M. Rusek, *J. Phys. Chem.* **1986**, *90*, 824.
[48] X. Zong, H. J. Yan, G. P. Wu, G. J. Ma, F. Y. Wen, L. Wang, C. Li, *J. Am. Chem. Soc.* **2008**, *130*, 7176.
[49] G. Williams, B. Seger, P. V. Kamat, *ACS Nano* **2008**, *2*, 1487.
[50] a) G. Williams, P. V. Kamat, *Langmuir* **2009**, *25*, 13869; b) K. P. Loh, Q. L. Bao, G. Eda, M. Chhowalla, *Nat. Chem.* **2010**, *2*, 1015.
[51] A. N. Cao, Z. Liu, S. S. Chu, M. H. Wu, Z. M. Ye, Z. W. Cai, Y. L. Chang, S. F. Wang, Q. H. Gong, Y. F. Liu, *Adv. Mater.* **2010**, *22*, 103.
[52] a) I. V. Lightcap, T. H. Kosel, P. V. Kamat, *Nano Lett.* **2010**, *10*, 577; b) C. L. Su, M. Acik, K. Takai, J. Lu, S.-j. Hao, Y. Zheng, P. P. Wu, Q. L. Bao, T. Enoki, Y. J. Chabal, K. P. Loh, *Nat. Commun.* **2012**, *3*, 1298.
[53] Y. H. Ng, A. Iwase, A. Kudo, R. Amal, *J. Phys. Chem. Lett.* **2010**, *1*, 2607.
[54] Y. H. Ng, I. V. Lightcap, K. Goodwin, M. Matsumura, P. V. Kamat, *J. Phys. Chem. Lett.* **2010**, *1*, 2222.
[55] Y. T. Liang, B. K. Vijayan, K. A. Gray, M. C. Hersam, *Nano Lett.* **2011**, *11*, 2865.
[56] X. Q. An, J. C. Yu, *RSC Adv.* **2011**, *1*, 1426.
[57] S. Morales-Torres, L. M. Pastrana-Martinez, J. L. Figueiredo, J. L. Faria, A. M. T. Silva, *Environ. Sci. Pollut. Res.* **2012**, *19*, 3676.
[58] Q. J. Xiang, J. G. Yu, M. Jaroniec, *Chem. Soc. Rev.* **2012**, *41*, 782.
[59] N. Zhang, Y. H. Zhang, Y. J. Xu, *Nanoscale* **2012**, *4*, 5792.
[60] J. S. Lee, K. H. You, C. B. Park, *Adv. Mater.* **2012**, *24*, 1084.
[61] H. Zhang, X. J. Lv, Y. M. Li, Y. Wang, J. H. Li, *ACS Nano* **2010**, *4*, 380.
[62] Q. Li, B. D. Guo, J. G. Yu, J. R. Ran, B. H. Zhang, H. J. Yan, J. R. Gong, *J. Am. Chem. Soc.* **2011**, *133*, 10878.
[63] R. Czerw, B. Foley, D. Tekleab, A. Rubio, P. M. Ajayan, D. L. Carroll, *Phys. Rev. B* **2002**, *66*, 033408.
[64] C. X. Guo, H. B. Yang, Z. M. Sheng, Z. S. Lu, Q. L. Song, C. M. Li, *Angew. Chem. Int. Ed.* **2010**, *49*, 3014.
[65] a) Y. Li, T. Sasaki, Y. Shimizu, N. Koshizaki, *J. Am. Chem. Soc.* **2008**, *130*, 14755; b) Y. Li, T. Sasaki, Y. Shimizu, N. Koshizaki, *Small* **2008**, *4*, 2286; c) Y. Xu, M. A. A. Schoonen, *Am. Mineral.* **2000**, *85*, 543.
[66] Q. J. Xiang, J. G. Yu, M. Jaroniec, *J. Phys. Chem. C* **2011**, *115*, 7355.
[67] K. K. Manga, Y. Zhou, Y. L. Yan, K. P. Loh, *Adv. Funct. Mater.* **2009**, *19*, 3638.
[68] N. Li, G. Liu, C. Zhen, F. Li, L. L. Zhang, H. M. Cheng, *Adv. Funct. Mater.* **2011**, *21*, 1717.
[69] Y. S. Fu, X. Wang, *Ind. Eng. Chem. Res.* **2011**, *50*, 7210.
[70] Y. H. Zhang, Z. R. Tang, X. Z. Fu, Y. J. Xu, *ACS Nano* **2010**, *4*, 7303.
[71] D. L. Zhao, G. D. Sheng, C. L. Chen, X. K. Wang, *Appl. Catal., B* **2012**, *111*, 303.
[72] J. C. Liu, H. W. Bai, Y. J. Wang, Z. Y. Liu, X. W. Zhang, D. D. Sun, *Adv. Funct. Mater.* **2010**, *20*, 4175.
[73] T. D. Nguyen-Phan, V. H. Pham, E. W. Shin, H. D. Pham, S. Kim, J. S. Chung, E. J. Kim, S. H. Hur, *Chem. Eng. J.* **2011**, *170*, 226.
[74] M. S. Zhu, P. L. Chen, M. H. Liu, *ACS Nano* **2011**, *5*, 4529.
[75] M. S. Zhu, P. L. Chen, M. H. Liu, *Langmuir* **2012**, *28*, 3385.
[76] I. Y. Kim, J. M. Lee, T. W. Kim, H. N. Kim, H. I. Kim, W. Choi, S. J. Hwang, *Small* **2012**, *8*, 1038.
[77] W. G. Tu, Y. Zhou, Q. Liu, Z. P. Tian, J. Gao, X. Y. Chen, H. T. Zhang, J. G. Liu, Z. G. Zou, *Adv. Funct. Mater.* **2012**, *22*, 1215.
[78] Y. Y. Liang, H. L. Wang, H. S. Casalongue, Z. Chen, H. J. Dai, *Nano Res.* **2010**, *3*, 701.
[79] B. J. Jiang, C. G. Tian, W. Zhou, J. Q. Wang, Y. Xie, Q. J. Pan, Z. Y. Ren, Y. Z. Dong, D. Fu, J. L. Han, H. G. Fu, *Chem. Eur. J.* **2011**, *17*, 8379.
[80] W. G. Tu, Y. Zhou, Q. Liu, S. C. Yan, S. S. Bao, X. Y. Wang, M. Xiao, Z. G. Zou, *Adv. Funct. Mater.* **2012**, *23*, 1743.
[81] H. L. Wang, J. T. Robinson, G. Diankov, H. J. Dai, *J. Am. Chem. Soc.* **2010**, *132*, 3270.
[82] W. S. Wang, D. H. Wang, W. G. Qu, L. Q. Lu, A. W. Xu, *J. Phys. Chem. C* **2012**, *116*, 19893.
[83] N. Zhang, Y. H. Zhang, X. Y. Pan, X. Z. Fu, S. Q. Liu, Y. J. Xu, *J. Phys. Chem. C* **2011**, *115*, 23501.
[84] E. P. Gao, W. Z. Wang, M. Shang, J. H. Xu, *Phys. Chem. Chem. Phys.* **2011**, *13*, 2887.
[85] S. Bai, X. P. Shen, X. Zhong, Y. Liu, G. X. Zhu, X. Xu, K. M. Chen, *Carbon* **2012**, *50*, 2337.
[86] Y. S. Fu, H. Q. Chen, X. Q. Sun, X. Wang, *Appl. Catal., B* **2012**, *111*, 280.
[87] Y. S. Fu, P. Xiong, H. Q. Chen, X. Q. Sun, X. Wang, *Ind. Eng. Chem. Res.* **2012**, *51*, 730.
[88] Y. S. Fu, Q. Chen, M. Y. He, Y. H. Wan, X. Q. Sun, H. Xia, X. Wang, *Ind. Eng. Chem. Res.* **2012**, *51*, 11700.
[89] Y. Fu, H. Chen, X. Sun, X. Wang, *AIChe. J.* **2012**, *58*, 3298.
[90] B. J. Li, H. Q. Cao, G. Yin, *J. Mater. Chem.* **2011**, *21*, 13765.
[91] C. H. Wu, Y. Z. Zhang, S. Li, H. J. Zheng, H. Wang, J. B. Liu, K. W. Li, H. Yan, *Chem. Eng. J.* **2011**, *178*, 468.
[92] S. Y. Song, W. Gao, X. Wang, X. Y. Li, D. P. Liu, Y. Xing, H. J. Zhang, *Dalton Trans.* **2012**, *41*, 10472.
[93] X. Tu, S. Luo, G. Chen, J. Li, *Chem. Eur. J.* **2012**, *18*, 14359.
[94] M. D. Hernandez-Alonso, F. Fresno, S. Suarez, J. M. Coronado, *Energ. Environ. Sci.* **2009**, *2*, 1231.
[95] T. F. Yeh, J. M. Syu, C. Cheng, T. H. Chang, H. S. Teng, *Adv. Funct. Mater.* **2010**, *20*, 2255.
[96] T. F. Yeh, F. F. Chan, C. T. Hsieh, H. S. Teng, *J. Phys. Chem. C* **2011**, *115*, 22587.
[97] X. Zhang, H. P. Li, X. L. Cui, Y. H. Lin, *J. Mater. Chem.* **2010**, *20*, 2801.
[98] W. Q. Fan, Q. H. Lai, Q. H. Zhang, Y. Wang, *J. Phys. Chem. C* **2011**, *115*, 10694.
[99] A. Beltran, J. R. Sambrano, M. Calatayud, F. R. Sensato, J. Andres, *Surf. Sci.* **2001**, *490*, 116.
[100] U. Diebold, *Surf. Sci. Rep.* **2003**, *48*, 53.
[101] Q. J. Xiang, J. G. Yu, M. Jaroniec, *Nanoscale* **2011**, *3*, 3670.
[102] Q. J. Xiang, J. G. Yu, M. Jaroniec, *J. Am. Chem. Soc.* **2012**, *134*, 6575.
[103] L. Jia, D. H. Wang, Y. X. Huang, A. W. Xu, H. Q. Yu, *J. Phys. Chem. C* **2011**, *115*, 11466.
[104] J. G. Hou, Z. Wang, W. B. Kan, S. Q. Jiao, H. M. Zhu, R. V. Kumar, *J. Mater. Chem.* **2012**, *22*, 7291.
[105] A. Mukherji, B. Seger, G. Q. Lu, L. Z. Wang, *ACS Nano* **2011**, *5*, 3483.

[106] J. Zhang, J. G. Yu, M. Jaroniec, J. R. Gong, *Nano Lett.* **2012**, *12*, 4584.
[107] P. D. Tran, S. K. Batabyal, S. S. Pramana, J. Barber, L. H. Wong, S. C. J. Loo, *Nanoscale* **2012**, *4*, 3875.
[108] A. Iwase, Y. H. Ng, Y. Ishiguro, A. Kudo, R. Amal, *J. Am. Chem. Soc.* **2011**, *133*, 11054.
[109] C. Chen, W. M. Cai, M. C. Long, B. X. Zhou, Y. H. Wu, D. Y. Wu, Y. J. Feng, *ACS Nano* **2010**, *4*, 6425.
[110] T. Kamegawa, D. Yamahana, H. Yamashita, *J. Phys. Chem. C* **2010**, *114*, 15049.
[111] L. L. Zhang, Z. G. Xiong, X. S. Zhao, *ACS Nano* **2010**, *4*, 7030.
[112] J. Du, X. Y. Lai, N. L. Yang, J. Zhai, D. Kisailus, F. B. Su, D. Wang, L. Jiang, *ACS Nano* **2011**, *5*, 590.
[113] Y. Fu, X. Sun, X. Wang, *Mater. Chem. Phys.* **2011**, *131*, 325.
[114] J. J. Guo, S. M. Zhu, Z. X. Chen, Y. Li, Z. Y. Yu, Q. L. Liu, J. B. Li, C. L. Feng, D. Zhang, *Ultrason. Sonochem.* **2011**, *18*, 1082.
[115] H. T. Hu, X. B. Wang, F. M. Liu, J. C. Wang, C. H. Xu, *Synth. Met.* **2011**, *161*, 404.
[116] B. J. Jiang, C. G. Tian, Q. J. Pan, Z. Jiang, J. Q. Wang, W. S. Yan, H. G. Fu, *J. Phys. Chem. C* **2011**, *115*, 23718.
[117] G. D. Jiang, Z. F. Lin, C. Chen, L. H. Zhu, Q. Chang, N. Wang, W. Wei, H. Q. Tang, *Carbon* **2011**, *49*, 2693.
[118] B. J. Li, H. Q. Cao, *J. Mater. Chem.* **2011**, *21*, 3346.
[119] B. J. Li, H. Q. Cao, G. Yin, Y. X. Lu, J. F. Yin, *J. Mater. Chem.* **2011**, *21*, 10645.
[120] C. B. Liu, Y. R. Teng, R. H. Liu, S. L. Luo, Y. H. Tang, L. Y. Chen, Q. Y. Cai, *Carbon* **2011**, *49*, 5312.
[121] J. C. Liu, L. Liu, H. W. Bai, Y. J. Wang, D. D. Sun, *Appl. Catal., B* **2011**, *106*, 76.
[122] T. Lv, L. K. Pan, X. J. Liu, T. Lu, G. Zhu, Z. Sun, *J. Alloys Compd.* **2011**, *509*, 10086.
[123] V. Stengl, D. Popelkova, P. Vlacil, *J. Phys. Chem. C* **2011**, *115*, 25209.
[124] F. Wang, K. Zhang, *J. Mol. Catal., A* **2011**, *345*, 101.
[125] Y. Y. Wen, H. M. Ding, Y. K. Shan, *Nanoscale* **2011**, *3*, 4411.
[126] T. G. Xu, L. W. Zhang, H. Y. Cheng, Y. F. Zhu, *Appl. Catal., B* **2011**, *101*, 382.
[127] Y. Yang, L. L. Ren, C. Zhang, S. Huang, T. X. Liu, *ACS. Appl. Mater. Interfaces* **2011**, *3*, 2779.
[128] D. H. Yoo, V. C. Tran, V. H. Pham, J. S. Chung, N. T. Khoa, E. J. Kim, S. H. Hahn, *Curr. Appl. Phys.* **2011**, *11*, 805.
[129] Q. Q. Zhai, T. Bo, G. X. Hu, *J. Hazard. Mater.* **2011**, *198*, 78.
[130] H. Zhang, X. F. Fan, X. Quan, S. Chen, H. T. Yu, *Environ. Sci. Technol.* **2011**, *45*, 5731.
[131] H. J. Zhang, P. P. Xu, G. D. Du, Z. W. Chen, K. Oh, D. Y. Pan, Z. Jiao, *Nano Res.* **2011**, *4*, 274.
[132] J. T. Zhang, Z. G. Xiong, X. S. Zhao, *J. Mater. Chem.* **2011**, *21*, 3634.
[133] X. F. Zhang, X. Quan, S. Chen, H. T. Yu, *Appl. Catal., B* **2011**, *105*, 237.
[134] Y. H. Zhang, Z. R. Tang, X. Fu, Y. J. Xu, *ACS Nano* **2011**, *5*, 7426.
[135] Y. P. Zhang, C. X. Pan, *J. Mater. Sci.* **2011**, *46*, 2622.
[136] F. Zhou, R. Shi, Y. F. Zhu, *J. Mol. Catal., A* **2011**, *340*, 77.
[137] K. F. Zhou, Y. H. Zhu, X. L. Yang, X. Jiang, C. Z. Li, *New J. Chem.* **2011**, *35*, 353.
[138] R. J. Zou, Z. Y. Zhang, L. Yu, Q. W. Tian, Z. G. Chen, J. Q. Hu, *Chem. Eur. J.* **2011**, *17*, 13912.
[139] P. Chen, T. Y. Xiao, H. H. Li, J. J. Yang, Z. Wang, H. B. Yao, S. H. Yu, *ACS Nano* **2012**, *6*, 712.
[140] Y. J. Cui, Z. X. Ding, P. Liu, M. Antonietti, X. Z. Fu, X. C. Wang, *Phys. Chem. Chem. Phys.* **2012**, *14*, 1455.
[141] D. Y. Fu, G. Y. Han, Y. Z. Chang, J. H. Dong, *Mater. Chem. Phys.* **2012**, *132*, 673.
[142] Z. Y. Gao, J. L. Liu, F. Xu, D. P. Wu, Z. L. Wu, K. Jiang, *Solid. State. Sci.* **2012**, *14*, 276.
[143] Z. Y. Gao, N. Liu, D. P. Wu, W. G. Tao, F. Xu, K. Jiang, *Appl. Surf. Sci.* **2012**, *258*, 2473.
[144] S. Ghasemi, S. R. Setayesh, A. Habibi-Yangjeh, M. R. Hormozi-Nezhad, M. R. Gholami, *J. Hazard. Mater.* **2012**, *199*, 170.
[145] C. Y. Hou, Q. H. Zhang, Y. G. Li, H. Z. Wang, *J. Hazard. Mater.* **2012**, *205*, 229.
[146] N. R. Khalid, Z. L. Hong, E. Ahmed, Y. W. Zhang, H. Chan, M. Ahmad, *Appl. Surf. Sci.* **2012**, *258*, 5827.
[147] C. H. Kim, B. H. Kim, K. S. Yang, *Carbon* **2012**, *50*, 2472.
[148] B. Li, T. Liu, Y. Wang, Z. Wang, *J. Colloid Interface Sci.* **2012**, *377*, 114.
[149] K. X. Li, Y. Huang, L. S. Yan, Y. H. Dai, K. P. Xue, H. Q. Guo, Z. M. Huang, J. J. Xiong, *Catal. Commun.* **2012**, *18*, 16.
[150] G. Z. Liao, S. Chen, X. Quan, H. T. Yu, H. M. Zhao, *J. Mater. Chem.* **2012**, *22*, 2721.
[151] B. T. Liu, Y. J. Huang, Y. Wen, L. J. Du, W. Zeng, Y. R. Shi, F. Zhang, G. Zhu, X. H. Xu, Y. H. Wang, *J. Mater. Chem.* **2012**, *22*, 7484.
[152] S. Liu, J. Q. Tian, L. Wang, Y. L. Luo, X. P. Sun, *Catal. Sci. Technol.* **2012**, *2*, 339.
[153] S. W. Liu, C. Liu, W. G. Wang, B. Cheng, J. G. Yu, *Nanoscale* **2012**, *4*, 3193.
[154] T. Lv, L. K. Pan, X. J. Liu, T. Lu, G. Zhu, Z. Sun, C. Q. Sun, *Catal. Sci. Technol.* **2012**, *2*, 754.
[155] Y. L. Min, K. Zhang, Y. C. Chen, Y. G. Zhang, *Sep. Purif. Technol.* **2012**, *86*, 98.
[156] B. Neppolian, A. Bruno, C. L. Bianchi, M. Ashokkumar, *Ultrason. Sonochem.* **2012**, *19*, 9.
[157] T. D. Nguyen-Phan, V. H. Pham, E. J. Kim, E. S. Oh, S. H. Hur, J. S. Chung, B. Lee, E. W. Shin, *Appl. Surf. Sci.* **2012**, *258*, 4551.
[158] T. D. Nguyen-Phan, V. H. Pham, H. Kweon, J. S. Chung, E. J. Kim, S. H. Hur, E. W. Shin, *J. Colloid Interface Sci.* **2012**, *367*, 139.
[159] S. D. Perera, R. G. Mariano, K. Vu, N. Nour, O. Seitz, Y. Chabal, K. J. Balkus, *ACS Catal.* **2012**, *2*, 949.
[160] P. Song, X. Y. Zhang, M. X. Sun, X. L. Cui, Y. H. Lin, *Nanoscale* **2012**, *4*, 1800.
[161] L. Sun, Z. L. Zhao, Y. C. Zhou, L. Liu, *Nanoscale* **2012**, *4*, 613.
[162] J. F. Wang, T. Tsuzuki, B. Tang, X. L. Hou, L. Sun, X. G. Wang, *ACS Appl. Mater. Interaces* **2012**, *4*, 3084.
[163] X. W. Wang, H. W. Tian, Y. Yang, H. Wang, S. M. Wang, W. T. Zheng, Y. C. Liu, *J. Alloys Compd.* **2012**, *524*, 5.
[164] A. H. Ye, W. Q. Fan, Q. H. Zhang, W. P. Deng, Y. Wang, *Catal. Sci. Technol.* **2012**, *2*, 969.
[165] D. H. Yoo, T. V. Cuong, V. H. Luan, N. T. Khoa, E. J. Kim, S. H. Hur, S. H. Hahn, *J. Phys. Chem. C* **2012**, *116*, 7180.
[166] X. Zhou, T. J. Shi, H. O. Zhou, *Appl. Surf. Sci.* **2012**, *258*, 6204.
[167] K. X. Zhu, L. W. Guo, J. J. Lin, W. C. Hao, J. Shang, Y. P. Jia, L. L. Chen, S. F. Jin, W. J. Wang, X. L. Chen, *Appl. Phys. Lett.* **2012**, 100.
[168] P. N. Zhu, A. S. Nair, S. J. Peng, S. Y. Yang, S. Ramakrishna, *ACS. Appl. Mater. Interfaces* **2012**, *4*, 581.
[169] S. J. Zhuo, M. W. Shao, S. T. Lee, *ACS Nano* **2012**, *6*, 1059.
[170] L. W. Zhang, H. B. Fu, Y. F. Zhu, *Adv. Funct. Mater.* **2008**, *18*, 2180.
[171] Y. J. Xu, Y. B. Zhuang, X. Z. Fu, *J. Phys. Chem. C* **2010**, *114*, 2669.
[172] Y. Yu, J. C. Yu, C. Y. Chan, Y. K. Che, J. C. Zhao, L. Ding, W. K. Ge, P. K. Wong, *Appl. Catal., B* **2005**, *61*, 1.
[173] E. Lee, J. Y. Hong, H. Kang, J. Jang, *J. Hazard. Mater.* **2012**, *219*, 13.
[174] N. Zhang, Y. Zhang, X. Pan, M.-Q. Yang, Y.-J. Xu, *J. Phys. Chem. C* **2012**, *116*, 18023.
[175] Y. H. Zhang, N. Zhang, Z. R. Tang, Y. J. Xu, *ACS Nano* **2012**, *6*, 9777.
[176] Y. Bi, S. Ouyang, N. Umezawa, J. Cao, J. Ye, *J. Am. Chem. Soc.* **2011**, *133*, 6490.
[177] Z. G. Yi, J. H. Ye, N. Kikugawa, T. Kako, S. X. Ouyang, H. Stuart-Williams, H. Yang, J. Y. Cao, W. J. Luo, Z. S. Li, Y. Liu, R. L. Withers, *Nat. Mater.* **2010**, *9*, 559.

[178] L. Liu, J. C. Liu, D. D. Sun, *Catal. Sci. Technol.* **2012**, *2*, 2525.
[179] Q. Liang, Y. Shi, W. Ma, Z. Li, X. Yang, *Phys. Chem. Chem. Phys.* **2012**, *14*, 15657.
[180] G. Liu, P. Niu, C. H. Sun, S. C. Smith, Z. G. Chen, G. Q. Lu, H. M. Cheng, *J. Am. Chem. Soc.* **2010**, *132*, 11642.
[181] S. Linic, P. Christopher, D. B. Ingram, *Nat. Mater.* **2011**, *10*, 911.
[182] S. C. Roy, O. K. Varghese, M. Paulose, C. A. Grimes, *ACS Nano* **2010**, *4*, 1259.
[183] M. R. Hoffmann, J. A. Moss, M. M. Baum, *Dalton Trans.* **2011**, *40*, 5151.
[184] Y. T. Liang, B. K. Vijayan, O. Lyandres, K. A. Gray, M. C. Hersam, *J. Phys. Chem. Lett.* **2012**, *3*, 1760.
[185] L. Li, G. D. Li, C. Yan, X. Y. Mu, X. L. Pan, X. X. Zou, K. X. Wang, J. S. Chen, *Angew. Chem. Int. Ed.* **2011**, *50*, 8299.
[186] X. J. Liu, L. K. Pan, T. Lv, T. Lu, G. Zhu, Z. Sun, C. Q. Sun, *Catal. Sci. Technol.* **2011**, *1*, 1189.
[187] X. J. Liu, L. K. Pan, T. Lv, G. Zhu, T. Lu, Z. Sun, C. Q. Sun, *RSC Adv.* **2011**, *1*, 1245.
[188] X. J. Liu, L. K. Pan, T. Lv, G. Zhu, Z. Sun, C. Q. Sun, *Chem. Commun.* **2011**, *47*, 11984.
[189] O. Akhavan, E. Ghaderi, *J. Phys. Chem. C* **2009**, *113*, 20214.
[190] O. Akhavan, M. Choobtashani, E. Ghaderi, *J. Phys. Chem. C* **2012**, *116*, 9653.
[191] Z. Hu, Y. D. Huang, S. F. Sun, W. C. Guan, Y. H. Yao, P. Y. Tang, C. Y. Li, *Carbon* **2012**, *50*, 994.
[192] P. Cheng, Z. Yang, H. Wang, W. Cheng, M. X. Chen, W. F. Shangguan, G. F. Ding, *Int. J. Hydrogen Energy* **2012**, *37*, 2224.
[193] H. I. Kim, G. H. Moon, D. Monllor-Satoca, Y. Park, W. Choi, *J. Phys. Chem. C* **2012**, *116*, 1535.
[194] X. J. Lv, W. F. Fu, H. X. Chang, H. Zhang, J. S. Cheng, G. J. Zhang, Y. Song, C. Y. Hu, J. H. Li, *J. Mater. Chem.* **2012**, *22*, 1539.
[195] Y. Park, S. H. Kang, W. Choi, *Phys. Chem. Chem. Phys.* **2011**, *13*, 9425.
[196] J. F. Shen, B. Yan, M. Shi, H. W. Ma, N. Li, M. X. Ye, *J. Mater. Chem.* **2011**, *21*, 3415.
[197] J. F. Shen, Y. Long, T. Li, M. Shi, N. Li, M. X. Ye, *Mater. Chem. Phys.* **2012**, *133*, 480.
[198] Z. Y. Wang, B. B. Huang, Y. Dai, Y. Y. Liu, X. Y. Zhang, X. Y. Qin, J. P. Wang, Z. K. Zheng, H. F. Cheng, *CrystEngComm* **2012**, *14*, 1687.
[199] P. Zeng, Q. G. Zhang, X. G. Zhang, T. Y. Peng, *J. Alloys Compd.* **2012**, *516*, 85.
[200] X. Y. Zhang, Y. J. Sun, X. L. Cui, Z. Y. Jiang, *Int. J. Hydrogen Energy* **2012**, *37*, 811.
[201] X. B. Meng, D. S. Geng, J. A. Liu, R. Y. Li, X. L. Sun, *Nanotechnology* **2011**, 22.
[202] X. Pan, Y. Zhao, S. Liu, C. L. Korzeniewski, S. Wang, Z. Y. Fan, *ACS. Appl. Mater. Interfaces* **2012**, *4*, 3944.
[203] N. R. Khalid, E. Ahmed, Z. L. Hong, Y. W. Zhang, M. Ahmad, *Curr. Appl. Phys.* **2012**, *12*, 1485.
[204] M. Shi, J. F. Shen, H. W. Ma, Z. Q. Li, X. Lu, N. Li, M. X. Ye, *Colloid Surf. A* **2012**, *405*, 30.
[205] J. H. Liu, Z. C. Wang, L. W. Liu, W. Chen, *Phys. Chem. Chem. Phys.* **2011**, *13*, 13216.
[206] M. S. A. S. Shah, A. R. Park, K. Zhang, J. H. Park, P. J. Yoo, *ACS Appl. Mater. Interfaces* **2012**, *4*, 3893.
[207] Y. Y. Gao, X. P. Pu, D. F. Zhang, G. Q. Ding, X. Shao, J. Ma, *Carbon* **2012**, *50*, 4093.
[208] L. M. Pastrana-Martinez, S. Morales-Torres, V. Likodimos, J. L. Figueiredo, J. L. Faria, P. Falaras, A. M. T. Silva, *Appl. Catal., B* **2012**, *123*, 241.
[209] Y. H. Zhang, N. Zhang, Z. R. Tang, Y. J. Xu, *Phys. Chem. Chem. Phys.* **2012**, *14*, 9167.
[210] Y. P. Zhang, J. J. Xu, Z. H. Sun, C. Z. Li, C. X. Pan, *Prog. Nat. Sci.* **2011**, *21*, 467.
[211] J. F. Shen, M. Shi, B. Yan, H. W. Ma, N. Li, M. X. Ye, *Nano Res.* **2011**, *4*, 795.
[212] Y. Lin, Z. G. Geng, H. B. Cai, L. Ma, J. Chen, J. Zeng, N. Pan, X. P. Wang, *Eur. J. Inorg. Chem.* **2012**, *28*, 4439.
[213] L. Ren, X. Qi, Y. D. Liu, Z. Y. Huang, X. L. Wei, J. Li, L. W. Yang, J. X. Zhong, *J. Mater. Chem.* **2012**, *22*, 11765.
[214] Y. C. Lee, J. W. Yang, *J. Ind. Eng. Chem.* **2012**, *18*, 1178.
[215] J. F. Wang, T. Tsuzuki, B. Tang, X. L. Hou, L. Sun, X. G. Wang, *ACS. Appl. Mater. Interfaces* **2012**, *4*, 3084.
[216] T. Kavitha, A. I. Gopalan, K. P. Lee, S. Y. Park, *Carbon* **2012**, *50*, 2994.
[217] Y. Liu, Y. Hu, M. J. Zhou, H. S. Qian, X. Hu, *Appl. Catal., B* **2012**, *125*, 425.
[218] D. G. Yin, L. Zhang, B. H. Liu, M. H. Wu, *J. Nanosci. Nanotechnol.* **2012**, *12*, 937.
[219] Q. Zhang, C. G. Tian, A. P. Wu, T. X. Tan, L. Sun, L. Wang, H. G. Fu, *J. Mater. Chem.* **2012**, *22*, 11778.
[220] Q. P. Luo, X. Y. Yu, B. X. Lei, H. Y. Chen, D. B. Kuang, C. Y. Su, *J. Phys. Chem. C* **2012**, *116*, 8111.
[221] T. Lv, L. K. Pan, X. J. Liu, Z. Sun, *Catal. Sci. Technol.* **2012**, *2*, 2297.
[222] X. J. Liu, L. K. Pan, Q. F. Zhao, T. Lv, G. Zhu, T. Q. Chen, T. Lu, Z. Sun, C. Q. Sun, *Chem. Eng. J.* **2012**, *183*, 238.
[223] P. Zeng, Q. G. Zhang, T. Y. Peng, X. H. Zhang, *Phys. Chem. Chem. Phys.* **2011**, *13*, 21496.
[224] P. Gao, J. Liu, S. Lee, T. Zhang, D. D. Sun, *J. Mater. Chem.* **2012**, *22*, 2292.
[225] S. G. Pan, X. H. Liu, *New J. Chem.* **2012**, *36*, 1781.
[226] S. X. Min, G. X. Lu, *J. Phys. Chem. C* **2012**, *116*, 25415.
[227] J. Guo, Y. Li, S. Zhu, Z. Chen, Q. Liu, D. Zhang, W.-J. Moon, D.-M. Song, *RSC Adv.* **2012**, *2*, 1356.
[228] Y. Hou, F. Zuo, A. Dagg, P. Y. Feng, *Nano Lett.* **2012**, *12*, 6464.
[229] Y. Hou, F. Zuo, Q. Ma, C. Wang, L. Bartels, P. Y. Feng, *J. Phys. Chem. C* **2012**, *116*, 20132.
[230] Z. Khan, T. R. Chetia, A. K. Vardhaman, D. Barpuzary, C. V. Sastri, M. Qureshi, *RSC Adv.* **2012**, *2*, 12122.
[231] H. Seema, K. C. Kemp, V. Chandra, K. S. Kim, *Nanotechnology* **2012**, *23*, 355705.
[232] L. Y. Chen, W. D. Zhang, B. Xu, Y. X. Yu, *J. Nanosci. Nanotechnol.* **2012**, *12*, 6921.
[233] X. Q. An, J. M. C. Yu, Y. Wang, Y. M. Hu, X. L. Yu, G. J. Zhang, *J. Mater. Chem.* **2012**, *22*, 8525.
[234] Y. W. Zhang, J. Q. Tian, H. Y. Li, L. Wang, X. Y. Qin, A. M. Asiri, A. O. Al-Youbi, X. P. Sun, *Langmuir* **2012**, *28*, 12893.
[235] Y. F. Sun, B. Y. Qu, Q. Liu, S. Gao, Z. X. Yan, W. S. Yan, B. C. Pan, S. Q. Wei, Y. Xie, *Nanoscale* **2012**, *4*, 3761.
[236] P. F. Wang, Y. H. Ao, C. Wang, J. Hou, J. Qian, *Carbon* **2012**, *50*, 5256.
[237] X. M. Zhang, X. F. Chang, M. A. Gondal, B. Zhang, Y. S. Liu, G. B. Ji, *Appl. Surf. Sci.* **2012**, *258*, 7826.
[238] F. D. Gao, D. W. Zeng, Q. W. Huang, S. Q. Tian, C. S. Xie, *Phys. Chem. Chem. Phys.* **2012**, *14*, 10572.
[239] X. J. Bai, L. Wang, Y. F. Zhu, *ACS Catal.* **2012**, *2*, 2769.
[240] X. L. Yu, G. J. Zhang, H. B. Cao, X. Q. An, Y. Wang, Z. J. Shu, X. L. An, F. Hua, *New J. Chem.* **2012**, *36*, 2593.
[241] Z. G. Xiong, L. L. Zhang, J. Z. Ma, X. S. Zhao, *Chem. Commun.* **2010**, *46*, 6099.